



Extracting accurate capacitance voltage curves from impedance spectroscopy

Kay-Michael Guenther, Hartmut Witte, Alois Krost, Stefan Kontermann, and Wolfgang Schade

Citation: [Applied Physics Letters](#) **100**, 042101 (2012); doi: 10.1063/1.3679380

View online: <http://dx.doi.org/10.1063/1.3679380>

View Table of Contents: <http://scitation.aip.org/content/aip/journal/apl/100/4?ver=pdfcov>

Published by the [AIP Publishing](#)

Articles you may be interested in

[General equivalent circuit derived from capacitance and impedance measurements performed on epitaxial ferroelectric thin films](#)

J. Appl. Phys. **116**, 044108 (2014); 10.1063/1.4891255

[Capacitances and energy deposition curve of nanosecond pulse surface dielectric barrier discharge plasma actuator](#)

Rev. Sci. Instrum. **85**, 053501 (2014); 10.1063/1.4871552

[Quantification of the specific membrane capacitance of single cells using a microfluidic device and impedance spectroscopy measurement](#)

Biomicrofluidics **6**, 034112 (2012); 10.1063/1.4746249

[Fast impedance spectroscopy: General aspects and performance study for single ion channel measurements](#)

Rev. Sci. Instrum. **71**, 2309 (2000); 10.1063/1.1150447

[Measurement of critical micelle concentration of nonionic surfactant solutions using impedance spectroscopy technique](#)

Rev. Sci. Instrum. **69**, 2514 (1998); 10.1063/1.1148951



AIP | Journal of
Applied Physics

Journal of Applied Physics is pleased to
announce **André Anders** as its new Editor-in-Chief

Extracting accurate capacitance voltage curves from impedance spectroscopy

Kay-Michael Guenther,^{1,a)} Hartmut Witte,² Alois Krost,² Stefan Kontermann,³ and Wolfgang Schade³

¹*Clausthal University of Technology, EFZN, Am Stollen 19B, 38640 Goslar, Germany*

²*Otto-von-Guericke University Magdeburg, Institute of Experimental Physics, Universitätsplatz 2, 39106 Magdeburg, Germany*

³*Fraunhofer Heinrich Hertz Institute, Am Stollen 19B, 38640 Goslar, Germany*

(Received 29 November 2011; accepted 5 January 2012; published online 24 January 2012)

We propose a method to obtain accurate capacitance-voltage (C - V) curves in the presence of multiple space charges. This method uses impedance spectroscopy to evaluate individual space charges separately. The advantage is that the knowledge of the exact equivalent circuit is not essentially needed. The comparison with other methods to calculate the doping concentration N_A shows that our method is unaffected by series resistances and agrees best with the correct value of N_A . The evaluation of the impedance spectra leads to a more thorough understanding of the respective Mott-Schottky plots. © 2012 American Institute of Physics. [doi:10.1063/1.3679380]

Evaluating capacitance-voltage (C - V) curves is a powerful tool to determine doping depth profiles of semiconductor materials¹ and other device parameters^{2,3} like the built-in voltage V_{bi} or oxide properties in metal-oxide-semiconductor structures.^{1,4} In short, the capacitance C of a reverse-biased Schottky diode is measured while varying the direct current (DC) bias voltage V_{DC} . The slope of the $1/C^2$ vs. V_{DC} plot, a so called Mott-Schottky-Plot, gives the effective doping density N_d at the respective bias voltage V_{DC} (Ref. 1)

$$N_d(V_{DC}) = \pm \frac{2}{q\epsilon_r\epsilon_0 A^2 d(1/C^2)/dV_{DC}}, \quad (1)$$

with the Schottky contact area A , the electron charge q , and the dielectric constant of the vacuum ϵ_0 and of the semiconductor material ϵ_r .

Commonly, the capacitance C of a sample is determined by interpreting a measured impedance $Z = R + iX$ using a suitable equivalent circuit¹ which is a combination of resistors R_x and capacitances C_x . The simplest equivalent circuit which can describe the behavior of a real sample is a parallel combination $R_p C_p$ in series with a resistor R_s .^{1,5} The RC combination represents the space charge region and R_s accounts for contact and bulk resistances.^{6,7} Unfortunately, this equivalent circuit cannot be obtained from a single impedance measurement at a fixed frequency. Instead, at least two measurements at two separate frequencies are needed.⁸ Then C_p , also called C_{2f} for distinction of this two-frequency-method, can be calculated using the relation

$$C_p = C_{2f} = \frac{1}{\omega_1^2 - \omega_2^2} \cdot \left(\frac{\omega_2}{X_2} - \frac{\omega_1}{X_1} \right), \quad (2)$$

which is not limited to any frequency range. However, Nara *et al.* suggest choosing ω_1 and ω_2 with care to minimize the calculation error in real applications.⁹ Conveniently, this

procedure is neglected, and a simple series or parallel connection of one capacitor and a single resistor is used instead, which is called $R_s C_s$ and $R_p C_p$, respectively.¹ Although having no counterpart in real samples, these equivalent circuits have the advantage that the capacitance can be calculated from a one-frequency impedance measurement⁵

$$C_s = -\frac{1}{\omega X}, \quad (3)$$

$$C_p = \left[-\frac{\omega R^2}{X} - \omega X \right]^{-1}. \quad (4)$$

Common impedance meters calculate these values automatically, but without additional calculations they can only be used in a very limited number of cases. Mostly, corrections have to be made afterwards,¹⁰ or the results must be interpreted with caution.^{11,12} For example, see the series resistance correction from Kavasoglu *et al.*¹⁰

As well as this one-frequency method, the previous two-frequency method only applies if additional space charges like pn-junctions or Schottky barriers are not present.⁹ Therefore, great care and extensive efforts are required to gain reliable data⁶ and often considerable assumptions and limitations are applied. This may lead to false results.

Hence, we generalize the two-frequency method for cases with intentionally present space charges, like a pn-junction. In such an experiment, the equivalent circuit can be assumed as a series of RC combinations with an additional series resistance R_s as shown in Fig. 1 with the impedance $Z(\omega)$

$$Z(\omega) = R_s + \sum_n \frac{R_n}{1 + \omega^2 R_n^2 C_n^2} - i \sum_n \frac{\omega R_n^2 C_n}{1 + \omega^2 R_n^2 C_n^2}. \quad (5)$$

The measured impedance depends on $2n+1$ parameters. Hence, corresponding to the two-frequency measurement, $2n+1$ measured frequencies ω_n would theoretically suffice, but such a method would be very impractical and time consuming due to extensive data analysis.

^{a)}Electronic mail: kay-michael.guenther@efzn.de. Phone: +49 5321 6855 170.

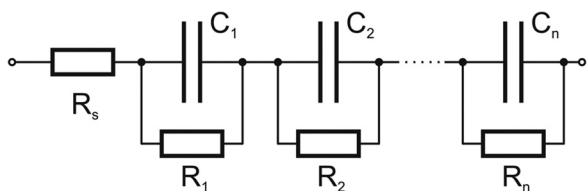


FIG. 1. Equivalent circuit for an arbitrary device with additional space charges.

Therefore, we propose a method which uses impedance spectroscopy. This technique determines the impedance Z as a function of the AC frequency ω and optional other parameters like the DC bias voltage V_{DC} . The resulting spectra $R(\omega)$ and $X(\omega)$ can be displayed and analyzed in Bode plots.⁵

The equivalent circuit in Fig. 1 produces for $n = 2$ a reactance spectrum as displayed in Fig. 2. For simplicity, the negative reactance $X(\omega)$ is used. Each RC combination produces a maximum in the negative reactance at its characteristic resonance frequency $\omega_{Ri} = 1/R_iC_i$ as shown by the dashed and dotted lines in Fig. 2. The peak height equals $R_i/2$. This information⁵ can also be extracted from the real part of Z , but the reactance has the advantage of being unaffected by the series resistance as can be seen from Eq. (5). The measured reactance spectrum results from the sum of each RC combination. This means, in theory, that the values for each RC combination, thus the capacitance C_n of each space charge region, can be extracted from one single spectrum simultaneously for the whole sample with

$$R_n = -2X(\omega_{Rn}), \tag{6}$$

$$C_n = \frac{1}{\omega_{Rn}R_n}. \tag{7}$$

It should be noted that an external DC voltage splits in voltage drops V_n which can be calculated from the direct current I_{DC} using the ohmic law $V_n = R_nI_{DC}$. When repeating this procedure for several bias voltages, the respective $C-V$ curves $C_n(V_n)$ can be determined.

In practice the measured reactance spectrum can appear as in Fig. 2, and the peaks are not clearly separated. To obtain all parameters, this curve has to be fitted, for example, with a complex nonlinear squares fit (CNLS),⁵ which can be difficult due to measurement errors. At this point, the great advantage of this method is that each RC combination can be

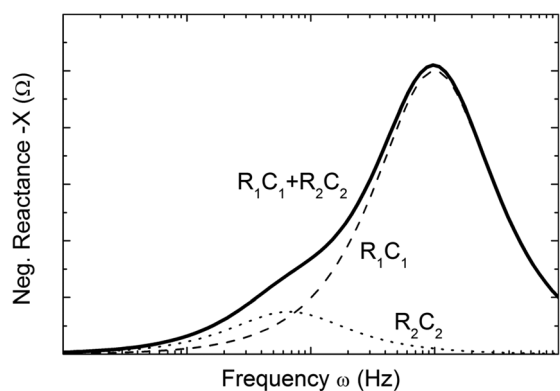


FIG. 2. Exemplary reactance spectra of two RC combinations (dashed and dotted) and their sum (solid).

analyzed independently from each other. For example, the solid curve in Fig. 2 could be the measurement of a semiconductor sample, whose doping profile has to be determined. Both metal contacts would obviously produce Schottky barriers. Nevertheless, in good approximation, the evaluation of the major peak yields the correct $C-V$ curve and therefore the correct doping profile.

To compare our method with conventional methods and demonstrate its advantages in difficult cases, we intentionally fabricate a semiconductor sample with two Schottky contacts by sputter coating 50 nm titanium followed by 150 nm gold through a shadow mask on top of a boron doped p-type float zone silicon wafer with a resistivity of 12–15 Ωcm as reported from the manufacturer. The sample is a quarter of a 4 in. wafer with a thickness of 280 μm . The contacts are rectangular with an interface area of 18.6 mm^2 and 14.6 mm^2 , respectively, and a distance of 4 mm (edge to edge). To avoid edge effects, the contacts have a distance of at least 10 mm from the sample edges. The impedance is measured using an Agilent E4980A Precision LCR Meter featuring a 10 mV AC amplitude, medium integration time, ten data acquisitions per step, and an internal DC bias source. Additionally, from a second quarter of the same wafer, we fabricate a sample with four annealed indium-zinc contacts in a van-der-Pauw arrangement for Hall effect measurements as reference. At room temperature, the current-voltage behavior is linear up to $I = 300 \mu\text{A}$, and surface depletion can be neglected. A resistivity of 12.5 Ωcm is calculated which is in

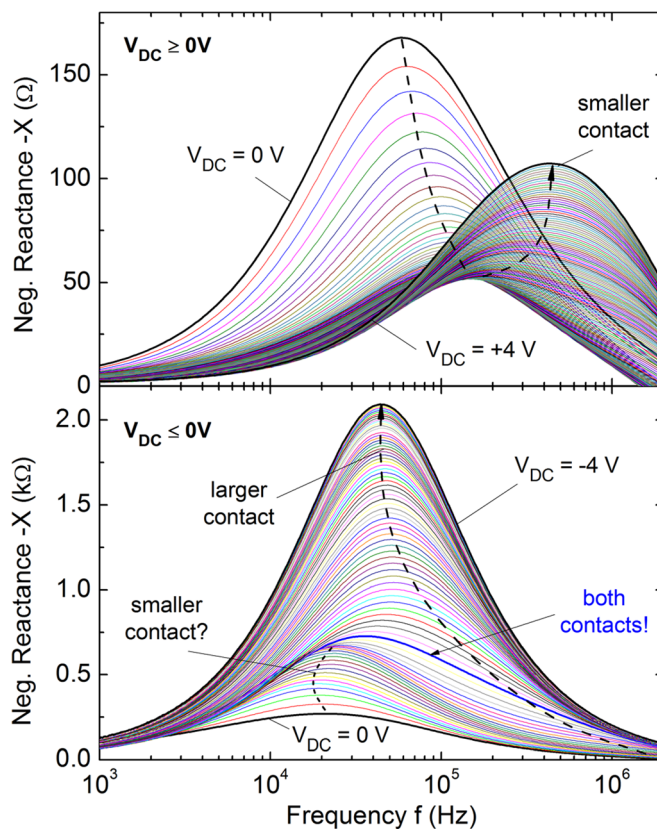


FIG. 3. (Color online) Reactance spectra of the sample for different DC bias voltages (voltage step $\Delta V_{DC} = 25 \text{ mV}$). For a better comprehension, positive ($V_{DC} = 0 \dots 4 \text{ V}$) and negative ($V_{DC} = -4 \dots 0 \text{ V}$) bias voltage variations are displayed separately. Dashed arrows indicate the dependence of reactance peaks on increasing DC voltage.

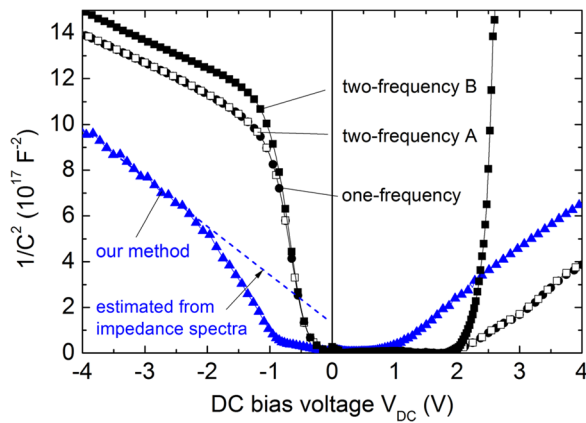


FIG. 4. (Color online) Mott-Schottky plots calculated from the reactance spectra using a one-frequency method (circles), the two-frequency method with two different frequency choices (open and solid squares), and a simple peak evaluation of the impedance spectra according to our technique (blue triangles). Deviations from the expected linear behavior around $V_{DC} = 0$ V are caused by incorrect capacitance values due to simultaneous impact of both Schottky contacts. A corrected behavior is estimated due to the reactance spectra.

good agreement with the manufacturer's value. The Hall effect measurement yielded a net doping density of $N_A = 1.72 \pm 0.03 \times 10^{15} \text{ cm}^{-3}$.

The resulting reactance spectra are shown in Fig. 3. For large positive or negative voltages (see dashed arrows in Fig. 3), one Schottky contact is in strong depletion while the other one is in strong accumulation. Hence, only one reactance peak is visible. The smaller contact is depleted for positive voltages and has its resonance frequency at approximately $\omega_R \approx 400$ kHz. The larger contact, however, depletes for negative voltages and produces a peak around $\omega_R \approx 40$ kHz. Equation (1) indicates that a larger contact interface area leads to a faster growth of the peak height with increasing voltages. Therefore, at the same absolute value of DC voltage, the peak heights differ by more than one order of magnitude. For smaller DC voltages, the contacts are not strongly depleted or accumulated. Hence, in this region both peaks can be observed simultaneously. In Fig. 3 this is shown exemplarily for the thick blue highlighted curve.

To compare the different methods for obtaining $C-V$ curves, we analyze the spectra from Fig. 3 with each method. The resulting $C-V$ curves are displayed in Fig. 4. The appropriate calculated acceptor concentrations can be found in Table I. The value from Hall measurements are used as a reference.

As an example for the one-frequency method, we calculate C_s using Eq. (3) and the impedance values at 1 MHz. For strong depletion, the resulting $C-V$ curve is approximately linear, and a linear fit yields the right order of magnitude for

the acceptor concentration with $N_A = 2.64 \dots 3.48 \times 10^{15} \text{ cm}^{-3}$. For lower voltages $|V_{DC}| < 1$ V, the approximation of a single capacitance no longer applies, and the curve should not be used for calculating the doping concentration, because it could easily be interpreted as a false doping profile. In fact, there are similarities to the $C-V$ curve of metal-insulator-semiconductor (MIS) structures.⁹ This would suggest a thin silicon oxide layer beneath the contacts which adds an additional RC combination to the equivalent circuit. Essentially, the theory for the one-frequency method cannot be applied.

For the two-frequency method the choice of the frequencies is crucial. Only under the assumption of a single capacitance the theory works with any frequency. This is not true for our sample. Therefore, no distinct $C-V$ curve can be calculated. Here, we used $\omega_1 = 1$ kHz and $\omega_2 = 2$ MHz for case A and $\omega_1 = 100$ kHz and $\omega_2 = 2$ MHz for case B to illustrate the problem. For case A the resulting curve and values for N_A in Table I are nearly identical to the one-frequency method. However, for case B the acceptor concentration is two orders of magnitude too small for positive DC voltages. Hence, the two-frequency method should only be used when additional space charges can definitely be excluded.

To test our method, we evaluate the reactance spectra from Fig. 3 by using a simple maximum value algorithm on the negative reactance. With Eqs. (6) and (7) and the ohmic law for the DC voltage correction we calculate the corresponding $C-V$ curve in Fig. 4. For strong depletion, the resulting acceptor concentrations show better agreement with the reference value than the other methods. Actually, the acceptor concentration $N_A = 1.61 \times 10^{15} \text{ cm}^{-3}$ for negative bias voltages is almost identical to the value from the Hall measurement. Additionally, the knowledge of the whole impedance spectra allows a better understanding of the $C-V$ curve for small DC voltages. For decreasing voltages, the resonance peak of the larger contact in Fig. 3 enters a regime where the resonance peak we assign to the smaller contact becomes visible. Due to the shifting dominance, the simple peak algorithm now takes the smaller contact for the calculation of the $C-V$ curve. Therefore, a change in the slope in Fig. 4 occurs at the respective voltage ($V_{DC} \approx -2$ V). As shown by the dashed blue line in Fig. 4, we assume a continuing linear behavior for the "larger contact" peak. A complete fit of the whole spectra should give the individual $C-V$ curve of each RC combination.

This comparison of methods proves that our method has many advantages over the conventional methods, which are only applicable under special circumstances. Our method can be applied in any cases where an equivalent circuit can be assumed as in Fig. 1 which includes the cases for the one- and two-frequency method.

TABLE I. Comparison of resulting acceptor concentrations N_A from single-frequency and two-frequency A and B analysis of the impedance and our method using impedance spectroscopy. All linear fits are performed at higher voltages ($|V_{DC}| > 2$ V) for positive and negative DC voltages. The value from Hall effect measurements is used as a reference.

| Method | Single-frequency N_A (10^{15} cm^{-3}) | Two-frequency A N_A (10^{15} cm^{-3}) | Two-frequency B N_A (10^{15} cm^{-3}) | Our method N_A (10^{15} cm^{-3}) | Hall effect (reference) N_A (10^{15} cm^{-3}) |
|-----------------|---|--|--|---|--|
| $V_{DC} < -2$ V | 2.64 ± 0.02 | 2.65 ± 0.02 | 2.81 ± 0.02 | 1.61 ± 0.06 | 1.72 ± 0.03 |
| $V_{DC} > +2$ V | 3.48 ± 0.02 | 3.40 ± 0.03 | 0.04 ± 0.002 | 2.77 ± 0.01 | 1.72 ± 0.03 |

We assume that the investigation of interface states or defects could be possible. Interface states can produce features in the impedance spectrum.^{3,13} This could explain the behavior around $V_{DC} = 0$ V where the impedance measurement is most sensitive to low impedance contributions. Alternatively, the reactance spectra can be interpreted with a MIS structure. The occurring peak around $V_{DC} = 0$ V could be associated with a thin oxide beneath the contacts. This would explain the resemblance of the resulting C - V curve with the characteristic behavior of a MIS structure.⁹ Fortunately, our method can be applied in both cases. Furthermore, our method may allow determining built-in voltages more accurately, because an exact C - V curve is the essential condition.¹⁰

In summary, we propose a method to calculate capacitance-voltage curves from impedance spectra. In theory, the capacitances of all space charges within a device can be evaluated simultaneously and independently from each other. Therefore, an exact equivalent circuit is not essentially needed but may improve the results. In comparison with traditional methods, our method proves to be unaffected by series resistances and gives a more accurate value for the depletion capacitance in the presence of additional space charges. We have shown that impedance spectroscopy

is a very powerful tool to understand Mott-Schottky plots in order to determine correct doping concentration profiles.

- ¹D. K. Schroder, *Semiconductor Material and Device Characterization* (John Wiley & Sons, New Jersey, 2006), pp. 61–109.
- ²A. S. Gudovskikh, J.-P. Kleider, J. Damon-Lacoste, P. Roca i Cabarrocas, Y. Veschetti, J.-C. Muller, P.-J. Ribeyron, and E. Rolland, *Thin Solid Films* **551–512**, 385 (2006).
- ³M. Adachi, M. Sakamoto, J. Jiu, Y. Ogata, and S. Isoda, *J. Phys. Chem. B* **110**, 13872 (2006).
- ⁴E. H. Nicollian, M. H. Hanes, and J. R. Brews, *IEEE Trans. Electron Devices* **20**, 380 (1973).
- ⁵E. Barsoukov and J. R. Macdonald, *Impedance Spectroscopy: Theory, Experiment, and Applications* (John Wiley & Sons, New Jersey, 2005).
- ⁶J. R. Shealy and R. J. Brown, *Appl. Phys. Lett.* **92**, 32101 (2008).
- ⁷R. Anil Kumar, M. S. Suresh, and J. Nagaraju, *Sol. Energy Mater. Sol. Cells* **60**, 155 (2000).
- ⁸J. F. Lonnum and J. S. Johannessen, *Electron. Lett.* **22**, 456 (1986).
- ⁹A. Nara, N. Yasuda, H. Satake, and A. Toriumi, *IEEE Trans. Semicond. Manuf.* **15**, 209 (2002).
- ¹⁰A. S. Kavasoglu, N. Kavasoglu, and S. Oktik, *Solid State Electron.* **52**, 990 (2008).
- ¹¹I. Mora-Sero, G. Garcia-Belmonte, P. P. Boix, M. A. Vazquez, and J. Bisquert, *Energy Environ. Sci.* **2**, 678 (2009).
- ¹²K. J. Yang and C. Hu, *IEEE Trans. Electron Devices* **46**, 1500 (1999).
- ¹³I. Mora-Sero, Y. Luo, G. Garcia-Belmonte, J. Bisquert, D. Munoz, C. Voz, J. Puigdollers, and R. Alcubilla, *Sol. Energy Mater. Sol. Cells* **92**, 505 (2008).